ASIAN JOURNAL OF PHARMACEUTICAL AND CLINICAL RESEARCH

INNOVARE ACADEMIC SCIENCES
Knowledge to Innovation

Vol 18, Issue 4, 2025

Online - 2455-3891
Print - 0974-2441

Research Article

EVALUATION OF ETHANOLIC EXTRACT OF *TILIACORA ACUMINATA* LEAVES FOR PANCREATIC LIPASE INHIBITION AND LIPID MODULATION: *IN SILICO* AND *IN VITRO* STUDIES

SHRIPRASANTH BHASKARAN, ANUSHA D*, KARTHIKA K, KAVITHA RAMASAMY

Department of Pharmacology, Sri Ramachandra Medical College and Research Institute, Chennai, Tamil Nadu, India.
***Corresponding author: Anusha D; Email: anusha.d@sriramachandra.edu.in**

Received: 11 January 2025, Revised and Accepted: 08 March 2025

ABSTRACT

Objectives: Hypercholesterolemia is a significant risk factor for cardiovascular disease and dyslipidemia. In 33–58% of individuals, current medications targeting 3-hydroxy-3-methyl-glutaryl-CoA reductase (HMGCR) and low-density lipoprotein (LDL) receptor do not intend to reduce LDL cholesterol. Pancreatic lipase, responsible for cholesterol absorption, can be a potential target in hypercholesterolemia. The current study aims to conduct virtual screening and molecular dynamics of compounds derived from ethanolic extract of *Tiliacora acuminata* leaves (TAL-EE) with pancreatic lipase, evaluate cell viability with 3-(4,5-dimethylthiazol-2-yl)-2,5-diphenyl tetrazolium (MTT) assay, assess lipase inhibition, perform lipid accumulation assessment (Oil Red O staining) and measure cholesterol and triglycerides (TG) in HepG2 cells.

Methods: Docking was carried out using AutoDock tools, and interaction analysis was performed with PyMOL 2.0. Para-nitrophenyl butyrate and porcine pancreatic lipase were used to test TAL-EE for lipase inhibition. Viability analysis (MTT test, IC_{50}), Oil Red O staining, and measurements of total cholesterol (TC) and triglyceride (TG) levels were conducted using HepG2 cells treated with TAL-EE.

Results: 5α-Androstan-16-one and cyclic ethylene mercaptole were identified through virtual screening to have the highest docking score (−9.4 kcaL/moL) for pancreatic lipase, exhibiting stability in dynamic studies. The IC_{50} for the 3-(4,5-dimethylthiazol-2-yl)-2,5-diphenyl tetrazolium (MTT) assay reported 20 µg/mL. After 48 h at lower doses, TAL-EE exhibited a 67% reduction of lipase activity and increased TG and TC levels in the medium of HepG2 cells, indicating reduced intracellular cholesterol levels.

Conclusion: TAL-EE showed significant pancreatic lipase inhibition and lipid modulation, suggesting potential as an antihypercholesterolemic agent.

Keywords: Tiliacora acuminata, Hypercholesterolemia, Pancreatic lipase, Lipid modulation.

 DOI: http://dx.doi.org/10.22159/ajpcr.2025v18i4.53932. Journal homepage: https://innovareacademics.in/journals/index.php/ajpcr

INTRODUCTION

Plants are a significant source of many modern medicines, and recent studies have increasingly examined the medicinal properties of various plant species [1]. There is a relationship between people and plants, and the study is termed ethnobotany [2]. The significance of biodiversity in the research and development of novel medicines is emphasized by ethnobotany, as over 700,000 plant species were found for therapeutic purposes [3]. Moreover, it promotes more efficacious and safe medicines [4] and ensures that traditional knowledge is backed by scientific research [5]. It emphasizes the integration of holistic concepts into modern medicine by promoting sustainable practices [6].

The *Tiliacora acuminata* (Lan) Hook. F and Thomas (Fig. 1) is a member of the *Menispermaceae* family. It is known as Bagmushda in Hindi, Perungattukodi in Tamil, and Krishnavetra in Sanskrit. It is a liana traditionally used for cancer management [7,8]. It is defined as a large, woody climber with cinereous, striate branches. The *Menispermaceae* family of plants contains yellow, elongated, lax, axillary, racemose panicles and long, oblong, acuminate, cordate, truncate, or rounded leaves. It is considered an antidote for snake bites in Ayurvedic medicine. It is found along river banks in many Indian states, including Tamil Nadu [9]. It has antibacterial, antidiarrheal, antioxidant, antiulcer, anti-inflammatory, antitumor, and immunostimulatory properties [10].

The cell membrane or plasma membrane consists of cholesterol, and it works as the immediate precursor for bile acids, steroid hormones, vitamin D, ubiquinol, and heme A [11]. Dyslipidemia is mainly due to hypercholesterolemia, characterized by high low-density lipoprotein (LDL) cholesterol, leading to an increased risk of cardiovascular diseases (CVD) [12,13]. Atherosclerosis also causes cholesterol accumulation in blood vessels and narrows arteries, leading to an increased risk of CVD and stroke [14]. It is essential to control cholesterol levels. Current treatments such as Statins and PCSK9 inhibitors are used for the management of dyslipidemia. Pancreatic lipase inhibitors are used in the management of obesity, which indirectly helps in the management of dyslipidemia. However, a considerable number of patients, about 33% to 58%, fail to achieve the desired LDL levels, and 5–30% of patients suffer from statin intolerance [15,16].

Moreover, current therapies using Statins primarily reduce cholesterol synthesis or absorption and cause elevated liver enzymes and drug interactions [17], while PCSK9 inhibitors like evolocumab and aliromumab modulate LDL receptors by an increase in excretion of LDL cholesterol from the bloodstream, but their higher costs and injectable form limit accessibility. Pancreatic lipase inhibitors like orlistat reduce lipid absorption and produce significant gastrointestinal side effects [11]. However, these therapies may not fully address the underlying causes of hypercholesterolemia [18]. Despite lowering the risk of CVD, these medications long-term effectiveness, tolerance, and metabolic differences underscore the importance of adopting a more comprehensive strategy.

The HepG2 cell lines generated from human liver cancer were used to study lipid metabolism and hypercholesterolemia. It expresses LDL receptors, helps to study lipid metabolism and cholesterol synthesis, and is used for testing lipid-modulating agents. HepG2 cell research

has improved our understanding of the mechanisms involved in liver metabolism disorders and helps in the assessment of possible therapies [19]. While prior studies [9] highlight the free radical scavenging and inflammatory reducing properties of the ethanolic extract of *T. acuminata* leaves, this research evaluates its pancreatic lipase inhibition and lipid modulation properties using HepG2 cells through *in silico* and *in vitro* approaches.

METHODS

Institutional Ethical Committee approved the study (CSP-MED/24/APR/i03/158). The study was conducted in the Department of Pharmacology of Sri Ramachandra Medical College and Research Institute, SRIHER, Chennai, Tamil Nadu, from June to August 2024.

Plant collection and validation

The leaves required for the study were obtained and validated by the Xavier Research Foundation at St. Xavier's College, Palayamkottai, Tamil Nadu, under certification number XCH-40567.

Study procedure

Molecular docking

A study of the ethanolic extract of *T. acuminata* leaves showed 13 components [9]. The component structures were acquired from the PubChem database, while the pancreatic lipase (1LPB) three-dimensional structure was purchased from the Protein Data Bank. Auto Dock Vina 1.1.2 is used for docking evaluation, and Auto Dock Tools 1.5.7 for protein and ligand preparation [20]. Ligand-protein interactions were displayed using PyMOL and the discovery studio visualizer [21]. After the virtual screening, the compound with the best docking score was picked, and its dynamic interactions with pancreatic lipase were explored using PyMOL 2.0.

Molecular dynamics (MD)

The structure's topology and coordinate parameters were created using the AMBERff19SB force field [22] and the LEAP module from the AmberTools22 package [23]. OPENMM software is used for MD simulation for 100 nanoseconds(ns) [24]. For neutralization of the complex, the structure was submerged using the TIP3P water model with a 10 Å buffer, and Na^+/Cl^- ions were introduced. Following 10,000 steps of energy minimization utilizing conjugate gradient and steepest descent techniques, the system was adjusted for 2 ns at 298 K and 1 atm in an NPT ensemble. The period of MD simulation for ligand-protein complexes was raised to 100 ns while maintaining the temperature at 300 K, the pressure at 1 bar, and the time step at 10 femtoseconds. Root Mean Square Deviation (RMSD) and Root Mean Square Fluctuation (RMSF) studies were done to assess conformational changes and intermolecular interactions. Principal Component Analysis (PCA) and Dynamic Cross-Correlation Matrix (DCCM) plots were generated using C^{++} trajectory analysis (CPPTRAJ) [25]. PyMOL (2.0, Schrödinger LLC) and Discovery Studio Visualizer (BIOVIA) served as tools in interaction experiments. Amber tool 22 was used to find the binding free energy.

Tiliacora acuminata leaves ethanolic extraction (TAL-EE)

The leaves of *T. acuminata* were extracted using ethanol using a Soxhlet system [26]. For 24 h, 100 g of dried *T. acuminata* leaf powder (Fig. 2a) was extracted using 250 mL of ethanol. After that, the extract (Fig. 2b) was dried and concentrated for use [9].

Determination of lipase inhibition

Porcine pancreatic lipase and para-nitrophenyl butyrate were purchased from Sigma Aldrich in the United States to assess lipid inhibition. The assay combination contained porcine pancreatic lipase prepared in 200 µl of 5 mg/ml enzyme preparation, 2 mM para-nitrophenyl butyrate, and 1 mL of distilled water with 50 mM sodium phosphate buffer (pH 8). After 30 min of incubation at 37°C, the reaction ended with 1 mL of sodium carbonate (10 mg/mL), and the assay mixture was measured at 430 nm [27]. Lipase activity was determined in the enzyme solution made in the buffer for inhibition tests following a 1/2-h incubation period. The kinetics of lipase inhibition were evaluated using para-nitrophenyl butyrate at doses ranging from 1 mm to 3 mm, both with and without MCT oil. The Dixon plots were used to calculate the inhibitory constant (Ki), and the Lineweaver-Burk (LB) plots were utilized to describe the kind of inhibition [28,29].

Fig. 1: *Tiliacora acuminata* (Lan) Hook. F and Thomas

Fig. 2: (a) *Tiliacora acuminata* leaves dry powder. (b) *Tiliacora acuminata* leaves ethanolic extract

MTT assay for the evaluation of cell viability

For this study, the HepG2 cell line was sourced from the National Centre for Cell Science, Pune. Sub-culture was done every 3 days with 5% Carbon dioxide and 18–20% Oxygen at 37°C on a minimum essential medium containing 10% fetal bovine serum (FBS) and 1% antibiotic-antimycotic solution [30] and used for MTT analysis to evaluate cytotoxicity and cell proliferation. Dulbecco's modified Eagle's Medium from Himedia Pvt Limited, dimethyl sulfoxide (DMSO) from Sigma-Aldrich, and FBS were used. The controls included were a negative control (cells devoid of the test chemical) and a medium control (no cells). To account for this interference, the same medium was utilized for both the control and test wells. A 96-well plate was seeded with 20,000 cells and incubated for 24 h. Test agents (1.25–40 µg/mL) were added. After which, another 24-h incubation was done with 5% carbon dioxide at 37°C. MTT reagent (0.5 mg/mL) was added for 3 h, formazan crystals were dissolved in DMSO, and an absorbance of 570 nm was measured [31-33]. Cell viability was calculated as follows:

$$\text{Percentage of cell viability} = \frac{\text{Mean absorbance (treated cells)}}{\text{Mean absorbance (untreated cells)}} \text{x}100$$

Lipid accumulation evaluation in HepG2 cells on TAL-EE

A 12-well plate was seeded with 1000 µL of cell suspension (20,000 cells/well) and cultivated for 24 h to reach 70% confluence to evaluate lipid accumulation in HepG2 cells. The test agent was administered with 0.1 mm oleic acid (OA) at doses of 2, 4, and 8 µg/mL. The cells were maintained for

an additional 48 h in 5% carbon dioxide at 37°C. The cells were incubated for 1 h and then fixed with a 4% paraformaldehyde solution in a phosphate-buffered saline (PBS). The samples were rinsed twice with PBS and treated with 60% isopropanol for 5 min. Following a 10-min incubation at room temperature with 1 mL of Oil Red O working stain, the samples were rinsed with distilled water and dried. Adding 100% isopropanol and gently swirling the liquid for 10 min eluted the Oil Red O stain color. The following formula was used to measure absorbance at 500 nm to quantify lipid accumulation:

$$\text{Percentage of Lipid accumulation} = \frac{\text{Mean OD of compound} + \text{OA} - \text{treated}}{\text{Mean OD of treated@500nm}} \text{X100}$$

Where: Optical density measures absorbance in treated (compound-exposed) and untreated (control) cells [34].

Estimation of total cholesterol (TC) and triglyceride (TG) in HepG2 cells treated with TAL-EE

To achieve 70% confluence, a 12-well plate was seeded with 1000 µL of cell suspension (20,000 HepG2 cells per well) and cultured for 24 h. After adding testing agents of 2, 4, and 8 µg/mL, the plates were incubated for 48 h in 5% carbon dioxide at 37°C. The TC and TG estimation kit was used to measure the levels of TC and TGs in the media [34].

Statistical analysis

Data were presented as mean±standard deviation. Statistical analysis was performed using Tukey's *post hoc* analysis, and a one-way analysis of variance was carried out using GraphPad Prism 8. $p<0.05$ were considered statistically significant.

RESULTS

***In silico* docking evaluation**

To evaluate the binding affinity to the pancreatic lipase enzyme, 13 compounds derived from the ethanolic extract of *T. acuminata* leaves identified from a previous study were selected [9]. The molecular docking analysis revealed varying binding affinities towards the enzymatic protein pancreatic lipase (Table 1). Through virtual screening, 5α-Androstan-16-one and cyclic ethylene mercaptole (ACEM) showed the highest binding score of −9.4 kcaL/moL, which prompted further dynamic studies to evaluate its stability and interaction with the target enzyme, pancreatic lipase.

The interaction analysis of ACEM and pancreatic lipase using docking and MDs simulations, illustrated in Fig. 3 and Table 2, yielded valuable insights. Docking revealed significant hydrogen bonds with residues such as Ala259, Arg256, and Asp79 (2.9–3.9 Å) and hydrophobic interactions with Phe215, His151, and Tyr114 (3.9–5.7 Å). MD simulations revealed hydrogen bonds with Asp80, Arg257, and Trp253 (2.9–3.9 Å), as well as hydrophobic interactions involving Ile79, Ala260, and Phe216 (4.3–5.1 Å).

Molecular Mechanics Generalized Born Surface Area (MMGBSA) (Table 3) evaluated the binding free energy (-25.63 kcal/mol) of the ACEM-Pancreatic lipase complex, indicating a stable and strong binding interaction. The Van der Waals interactions (VdW) contributed significantly with -31.1 kcal/mol, and electrostatic interactions (EEL) were favorable at -1.24 kcal/mol. Although the desolvation effect (EGB) was positive at 10.57 kcal/mol, the negative surface area solvation energy (ESURF) of -3.86 kcal/mol helped to mitigate the effects. The Gas-phase free energy (ΔGgas) of -35.35 kcal/mol further reinforced the strong binding.

To enhance the significance of MDs, the key parameters like The RMSD (Fig. 4a) stabilized between 1.5 Å and 2.0 Å after an initial equilibration phase, with a prominent peak at 1.5 Å, confirming structural stability throughout the simulation. The 2D-RMSD plot (Fig. 4b) displayed uniform deviations over time, indicating consistent structural similarity throughout the analysis. The RMSF analysis (Fig. 4c) showed low fluctuations below 1.5 Å for most residues, indicating

Table 1: Ligands that bind to the protein pancreatic lipase exhibit varying binding energies

S. No.	Drug	Pancreatic lipase (kcaL/moL)	S. No.	Drug	Pancreatic lipase (kcaL/moL)
1	3,7,11,15-Tetramethyl-2- hexadecen-1-ol	−5.5	8.	9,12,15-Octadecatrienoic acid, (Z, Z, Z)	−5.8
2	Cyclopentaneundecanoic acid, methyl ester	−6.0	9.	1-Iodo-2-methylundecane	−5.3
3	Hexadecanoic Acid, Ethyl Ester	−5.6	10.	1-Iodo-2-methylnonane	−4.8
4	9,12-Octadecadienoic Acid, Methyl Ester,	−5.5	11.	Heptadecane, 2,6-dimethyl-	−6.2
5	9,12,15-Octadecatrienoic acid, methyl ester, (Z, Z, Z)-	−5.5	12.	Squalene	−7.9
6	9,12,15-Octadecatrienoic acid, methyl ester, (Z, Z, Z)-	−6.2	13.	5α-Androstan-16-one, cyclic ethylene mercaptole (ACEM)	−9.4
7.	9,12-Octadecadienoic acid (Z, Z)	−6.1			

Table 2: Intermolecular interactions in 5α-Androstan-16-one, cyclic ethylene mercaptole -Pancreatic lipase complex

Protein/ligand complex	Docking/MD	Interacting amino acid residues (Distance Å)	
		Hydrogen bond	Hydrophobic interaction
ACEM- Pancreatic lipase complex	Docking	Ala259 (3.9), Arg256 (3.9), Asp79 (3.1), Phe77 (2.9)	Phe215 (3.9), His151 (5.7), His263 (5.4), Ile78 (4.9), Ala260 (4.5), Leu264 (4.6), Phe77 (4.7), Tyr114 (4.5)
	Molecular dynamics	Asp80 (2.9), Arg257 (3.4), Phe78 (3.1), Trp253 (3.9)	Ile79 (4.6), Arg257 (4.3), Ala260 (4.9), Ala261 (4.8), Phe216 (4.7), Trp253 (5.1)

Table 3: Molecular mechanics generalized born surface area binding free energy of 5α-Androstan-16-one, cyclic ethylene mercaptole- lipase complex

Protein/ligand complex	VdW	EEL	EGB	ESURF	Δ Ggas	Δ Gsolv	Δ G Bind
ACEM-pancreatic lipase complex	−31.1	−1.24	10.57	−3.86	−35.35	6.71	−25.63

ACEM: 5α-Androstan-16-one and cyclic ethylene mercaptole

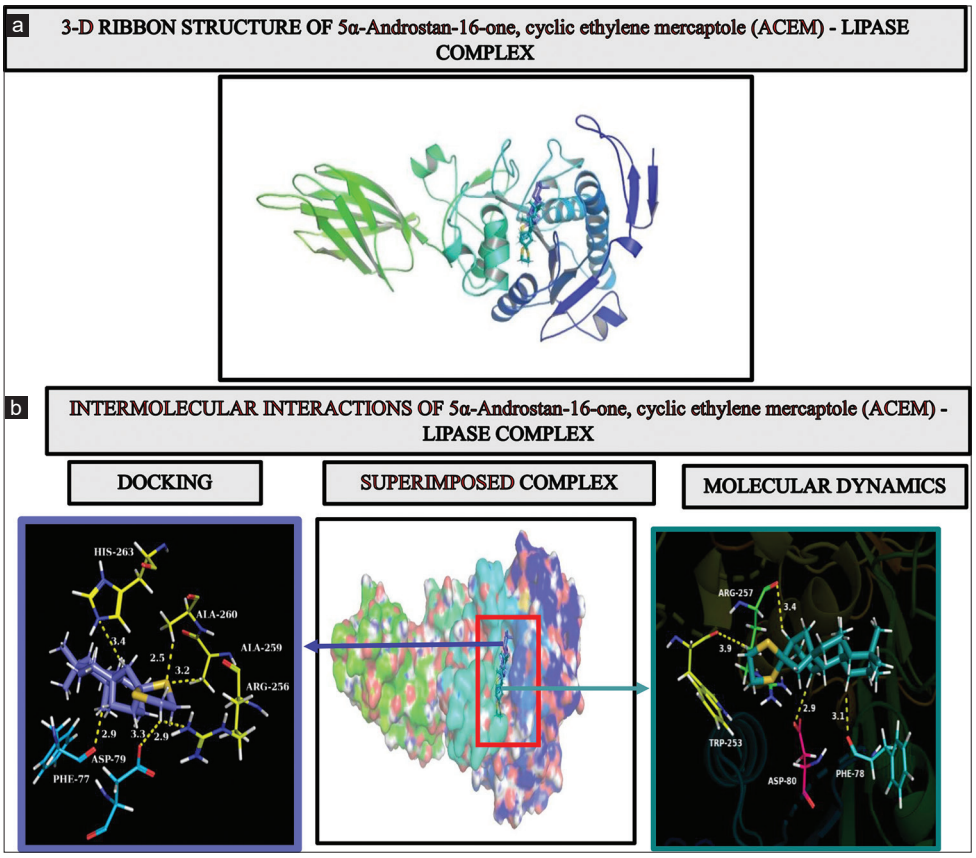

Fig. 3: (a) 3-D Ribbon structure of 5α-Androstan-16-one, cyclic ethylene mercaptole (ACEM) binding to pancreatic lipase (b) Intermolecular interactions of ACEM-lipase enzyme complex at the end of docking and molecular dynamics (MD) simulation. The Superimposed structure of ACEM-Lipase complex of docking is depicted in blue and MDs are depicted in cyan green

rigidity. At the same time, peaks in the flexible regions, such as loops and termini, highlighted their dynamic nature. The radius of gyration (Fig. 4d) remained stable, ranging from 25.2 Å to 26.6 Å, with a peak at 25.8 Å, demonstrating that the structure maintained compactness. The dynamic cross-correlation matrix (Fig. 4e) displayed strong self-correlations (purple diagonal) and off-diagonal clusters of positive (purple) and negative (green) correlations, indicating coordinated and anti-coordinated motions between residue pairs. PCA (Fig. 4f) further revealed that the system explored a confined conformational space with minimal large-scale changes, supporting the overall stability observed. The unimodal distributions of PC1 and PC2 indicated smooth transitions and minimal large-scale conformational changes, reflecting structural stability during the simulation.

Determination of pancreatic lipase inhibition of TAL-EE

An overview of the pancreatic lipase enzyme inhibition study result is given in Table 4. TAL-EE demonstrated dose-dependent inhibition of lipase activity (Fig. 5), a 67% reduction was observed at a concentration of 2 mg/mL. The IC_{50} value of TAL-EE against pancreatic lipase was found to be 1.47 mg/mL. The LB plot (Fig. 6) revealed that TAL-EE inhibited lipase through a non-competitive mechanism, and the Dixon plot (Fig. 7) showed that the inhibition constant (Ki) for TAL-EE was 828.46 µg/mL.

MTT-based cell viability evaluation

The MTT test results (Table 5 and Fig. 8) showed a concentration-dependent reduction in cell viability. At 1.25 µg/mL, viability was 97.14%, indicating minimal impact. Viability declined with increasing concentrations, reaching 71.79% at 10 µg/mL and 50.53% at the IC_{50} value of 20 µg/mL. At 40 µg/mL, viability dropped significantly to 15.78%. These results indicated low cytotoxicity at lower concentrations, with increasing effects at higher doses. Microscopic observations of TAL-EE-treated cells after 24 h (Fig. 9) further highlighted the compound's impact.

Table 4: Overview of results obtained for pancreatic lipase inhibition

Enzyme activity	IC_{50} (mg/mL)	Type of inhibition	Ki (µg/mL)
Lipase	1.47	Non-competitive	828.46

Lipid accumulation evaluation in HepG2 cells on TAL-EE

HepG2 cell lines treated with varying concentrations of TAL-EE (2, 4, and 8 µg/mL) for 24 h showed a significant reduction in lipid accumulation induced by OA. This reduction was observed to increase with higher concentrations, as illustrated in Fig. 10 and Table 6. Additionally, Oil Red O staining revealed a noticeable decrease in lipid deposition with an increase in concentration, providing clear visual evidence of the extract's lipid-modulating effects (Fig. 11).

TC and TG estimation

Treatment of HepG2 cells for 48 h with TAL-EE has enhanced the secretion of TGs and TC into the extracellular medium from HepG2 cells with an increase in the concentration of the TAL-EE extract. This indicates a potential modulatory effect of TAL-EE on lipid metabolism in HepG2 cells, as illustrated in (Fig. 12a and b) and Table 7.

DISCUSSION

Management of hypercholesterolemia is very crucial as it is not only a major risk factor for CVD but also genetic disorders (familial hypercholesterolemia) and other metabolic disorders. Current therapies can lead to adverse effects and treatment failures. Additionally, the variability in patient responses due to factors such as genetics, age, and lifestyle presents an opportunity for new management approaches [35].

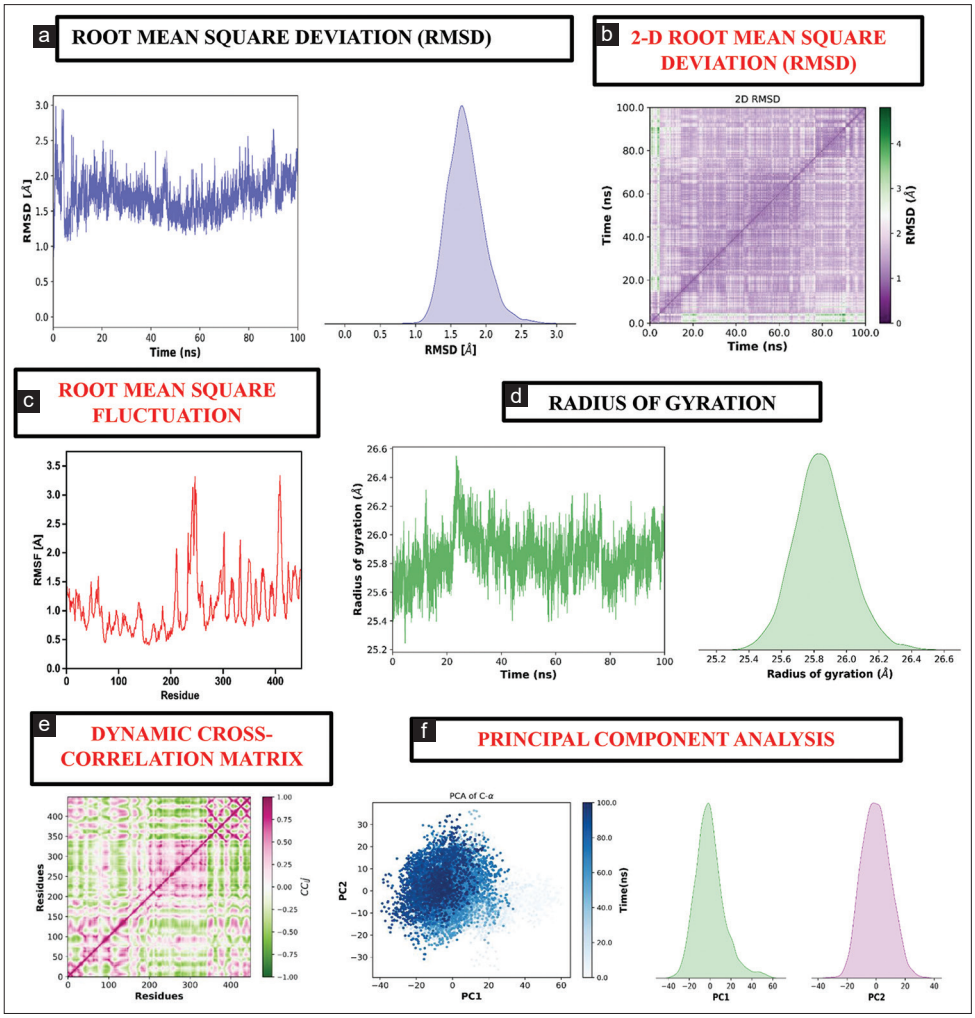

Fig. 4: Plots of ACEM- Pancreatic lipase enzyme complex (a). Root Mean Square Deviation (RMSD) (b). 2D- Root Mean Square Deviation (RMSD) (c). Root mean square Fluctuation (RMSF) (d). Radius of Gyration (e). Dynamic cross-correlation matrix (DCCM) (f). Principal Component Analysis (PCA).

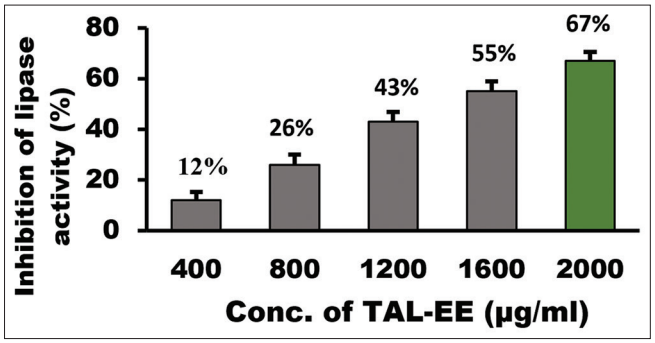

Fig. 5: Inhibition of pancreatic lipase by *Tiliacora acuminata* leaves ethanolic extraction. Statistical values are expressed as mean±SD and converted to percentages

T. acuminata is known for its medicinal properties, as mentioned in [7-9,36-38]. The hypocholesterolemic properties of *T. acuminata* have been underexplored. This study was initiated because *Tiliacora triandra*, belonging to the same family, has shown significant pancreatic lipase inhibitory activity and lipid modulation [39,40]. Various plant-based compounds have also been identified as pancreatic lipase inhibitors like *Panax ginseng* saponin extracts, Fenugreek seeds, rich in saponins, ginger extract, green tea catechins, and olive leaf extract have shown pancreatic lipase inhibition [41-45].

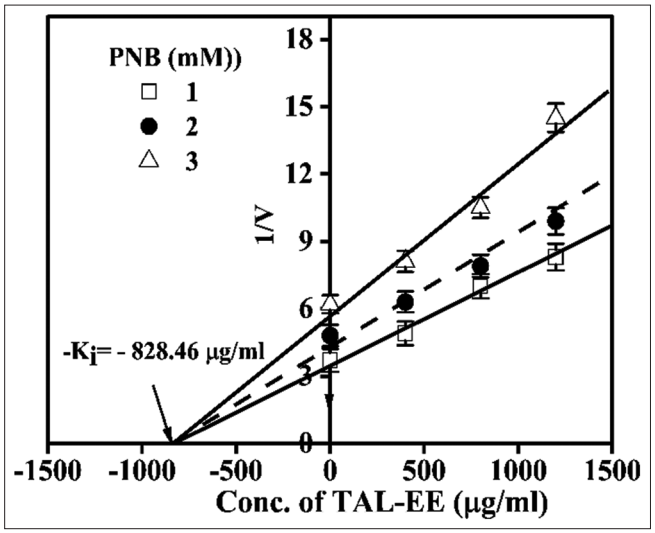

Fig. 6: Lineweaver-Burk plot of pancreatic lipase inhibition by *Tiliacora acuminata* leaves ethanolic extraction

On virtual screening, out of 13 constituents from the ethanolic extract of *T. acuminata* leaves (TAL-EE) (Table 1), ACEM showed the highest docking score, indicating the most substantial potential for interaction

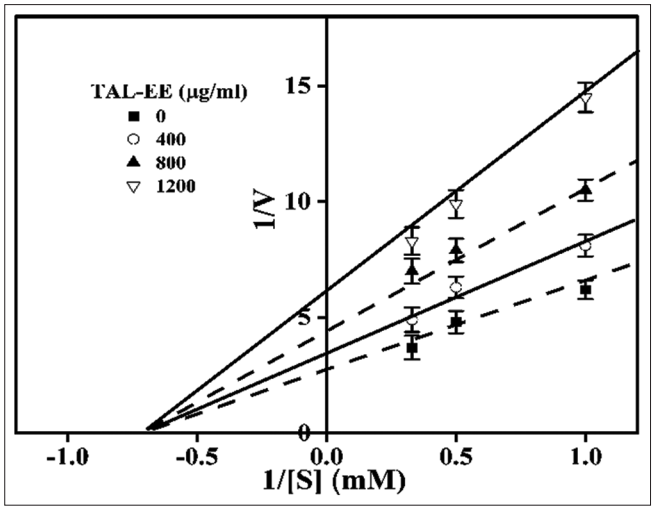

Fig. 7: Dixon plot of pancreatic lipase inhibition by *Tiliacora acuminata* leaves ethanolic extraction

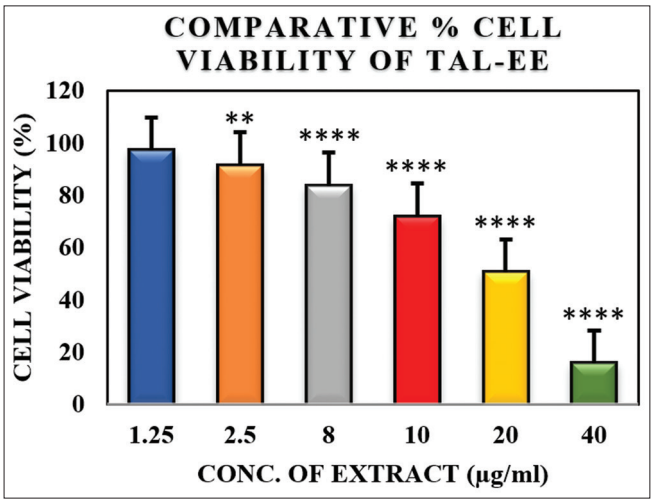

Fig. 8: Comparative percentage cell viability at various concentrations of *Tiliacora acuminata* leaves ethanolic extraction. Statistical values are expressed as mean±SD and converted to percentages. A p<0.01 is indicated by **. While ****p<0.0001, compared to control cells, demonstrating statistical significance (p<0.05).

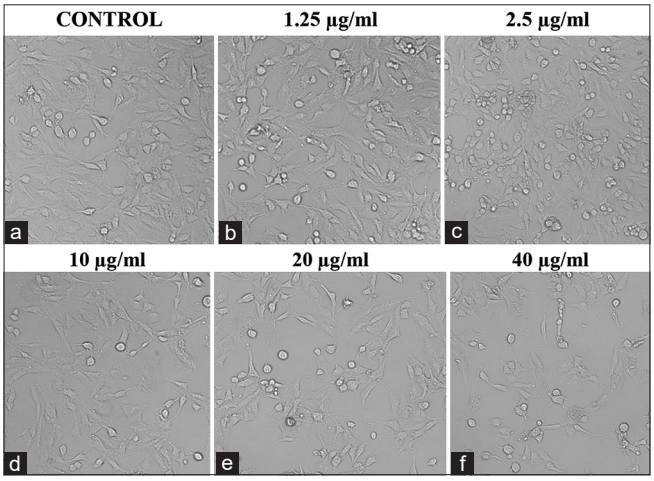

Fig. 9: Microscopic observations of *Tiliacora acuminata* leaves ethanolic extraction-treated cells after 24 h. (a) Control. (b) 1.25 µg/mL. (c) 2.5 µg/mL. (d) 10 µg/mL. (e) 20 µg/mL. (f) 40 µg/mL

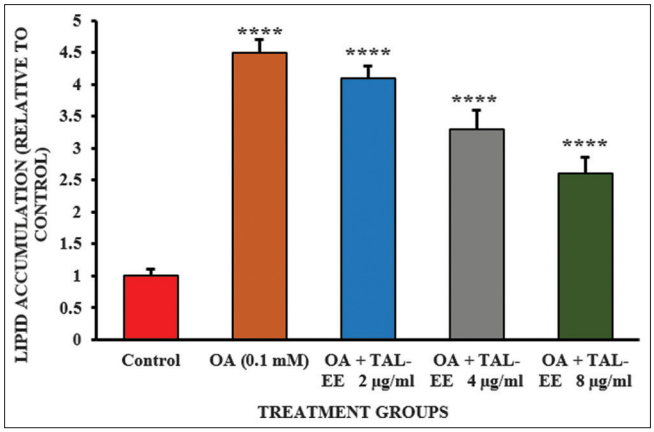

Fig. 10: Effect of *Tiliacora acuminata* leaves ethanolic extraction on lipid accumulation in HepG2 cells. Statistical values are expressed as mean±SD and converted to percentages. ****p<0.0001, compared to control cells, demonstrating statistical significance (p<0.05)

Table 5: Cell viability at various concentrations of TAL-EE

Summary-MTT assay		IC50 value
Concentration of TAL-EE (µg/mL)	% cell viability	
Untreated	100	20 µg/mL
1.25	97.14	
2.5	91.41	
8	83.65	
10	71.79	
20	50.53	
40	15.78	

TAL-EE: *Tiliacora acuminata* leaves ethanolic extraction, MTT: 3-(4,5-dimethylthiazol-2-yl)-2,5-diphenyl tetrazolium

Table 6: Effect of TAL-EE on lipid accumulation in HepG2 cells. Statistical values are presented as mean±SD

Groups	Lipid accumulation (relative to control)	Standard deviation
Control	1	0.1
OA (0.1 mm)	4.5	0.2
OA+TAL-EE 2 µg/mL	4.1	0.19
OA+TAL-EE 4 µg/mL	3.3	0.3
OA+TAL-EE 8 µg/mL	2.6	0.26

TAL-EE: *Tiliacora acuminata* leaves ethanolic extraction, OA: Oleic acid

with the Pancreatic lipase enzyme. MDs simulations confirmed the stable binding of ACEM within the pancreatic enzyme's active site (Table 2 and Fig. 3). The primary interactions involved Trp253, which provided excellent binding stability, and Ala260, which ensured strong ligand contact. The binding free energy of the ACEM-pancreatic lipase complex (Table 3) also confirmed the stable and strong binding interaction. The RMSD, RMSF, radius of gyration, prostate-specific antigen analysis, and DCCM (Fig. 4a-f) confirmed the stability interactions throughout the simulation.

TAL-EE demonstrated high binding affinity and significant non-competitive pancreatic lipase inhibition, achieving a 67% reduction at 2 mg/mL as determined by the LB plot and Dixon plot (Table 4 and Figs. 5-7). Various studies using lemon basil seed-derived peptides and de-oiled rice bran peptides exhibited the same method of pancreatic lipase inhibition [46-48]. These results showed TAL-EE's potential in lipid disorders by inhibiting pancreatic lipase.

Table 7: Total cholesterol estimation and triglyceride estimation. Statistical values are presented as mean±SD

Groups	Total cholesterol (mm)	Standard deviation	Triglycerides (mm)	Standard deviation
Control	0.015	0.009	0.026	0.009
TAL-EE 2 µg/mL	0.032	0.01	0.09	0.01
TAL-EE 4 µg/mL	0.049	0.014	0.15	0.014
TAL-EE 8 µg/mL	0.08	0.018	0.2	0.018

TAL-EE: *Tiliacora acuminata* leaves ethanolic extraction

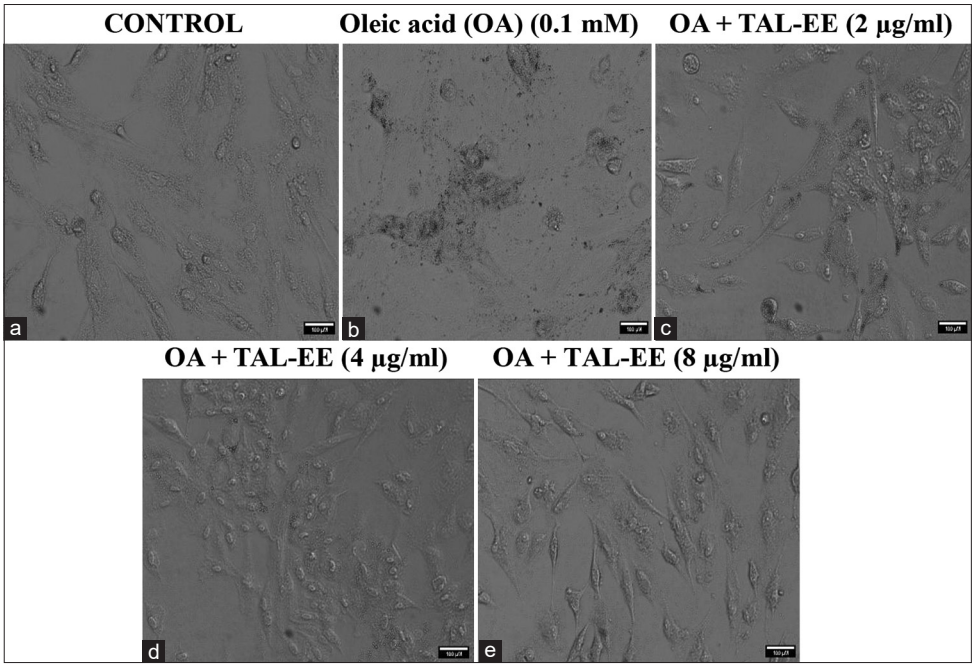

Fig. 11: Representative images showing the oil red O staining of HepG2 cells treated with *Tiliacora acuminata* leaves ethanolic extraction at various concentrations (2 µg/mL, 4 µg/mL, and 8 µg/mL). (a) Control. (b) Oleic acid (0.1 mM). (c) OA + TAL-EE (2 µg/mL). (d) OA + TAL-EE (4 µg/mL). (e) OA + TAL-EE (8 µg/mL)

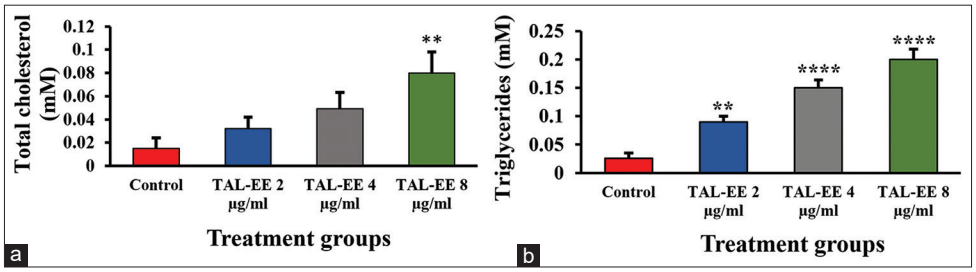

Fig. 12: (a) The effect of *Tiliacora acuminata* leaves ethanolic extraction (TAL-EE) on the secretion of total cholesterol in HepG2 cells. **p<0.01 compared to control cells (b) The effect of TAL-EE on the secretion of triglycerides in HepG2 cells. ****p<0.0001 compared to control cells, statistical values are expressed as mean±SD. Both (a) and (b), indicating statistically significant (p<0.05)

The MTT assay results of TAL-EE (Table 5 and Fig. 8) showed a significant concentration-dependent decrease in HepG2 cell viability. Highly significant effects were recorded for concentrations above 4 µg/mL ($p<0.05$), showing TAL-EE's concentration-dependent cytotoxicity, similar to the results of Vakele *et al*. [46]. TAL-EE also showed significant modulation of lipid metabolism at lower concentrations with minimal cytotoxic effects, similar to the study by Tie *et al*. [49] in which kaempferol and kaempferide were found to modulate lipid metabolism at low concentrations.

Treatment of TAL-EE on OA -induced HepG2 cells, as described in Cui *et al*. [50], showed a significant reduction in lipid accumulation in a concentration-dependent manner (Table 6 and Fig. 10). However, lipid levels at 8 µg/mL in treated groups remained above the control, indicating potential effectiveness but necessitating further research for optimization. According to Oil Red O staining in Fig. 11, an increase in concentration resulted in a decrease in lipid deposition within the cell. TAL-EE also increased the secretion of TC and TG from HepG2 cells on the increase in concentration significantly, like similar methods used by green tea catechins to regulate lipid metabolism [51].

CONCLUSION

In this study, the *T. acuminata* leaves - ethanolic extract (TAL-EE) showed a highly significant concentration-dependent pancreatic lipase inhibitory activity. TAL-EE also showed a significant reduction in lipid accumulation and increased TG and cholesterol secretion in HepG2 cells. This suggests that the TAL-EE could serve as a potential natural compound for the management of hypercholesterolemia and

other lipid-related disorders. Further animal studies are required to validate its therapeutic efficacy and safety.

ACKNOWLEDGMENT

We would like to thank the Department of Pharmacology, Sri Ramachandra Medical College and Research Institute, for providing the facilities to complete this research.

AUTHORS CONTRIBUTION

All authors contributed equally to this work. The authors confirm the contributions to the paper as follows: Study conception and design by SHRIPRASANTH BHASKARAN, Data analysis and interpretation of results by D. ANUSHA, Draft preparation by K. KARTHIKA, and Draft Manuscript guidance by KAVITHA RAMASAMY. The final version of the manuscript was approved by all authors after they had examined the findings.

CONFLICT OF INTEREST

The authors declare that there are no conflicts of interest.

FUNDING

Nil.

REFERENCES

1. Pradeepa M, Ramesh R, Thirumurugan K. Qualitative and quantitative phytochemical analysis and bactericidal activity of *Pelargonium graveolens* L'Her. Indian J Appl Pharm Sci. 2016;8(3):7-11. doi: 10.22159/ijap.2016v8i3.9075
2. McClatchey WC, Mahady GB, Bennett BC, Shiels L, Savo V. Ethnobotany as a pharmacological research tool and recent developments in CNS-active natural products from ethnobotanical sources. Pharmacol Ther. 2009 Aug;123(2):239-54. doi: 10.1016/j.pharmthera.2009.04.002, PMID 19422851, PMCID PMC2700180
3. Purohit SP, Jugran AK, Bhatt ID, Palni LM, Bhatt AB, Nandi SK. *In Vitro* Approaches for Conservation and Reducing Juvenility of *Zanthoxylum Armatum* DC: An Endangered Medicinal Plant of Himalayan Region-Trees. Springer Berlin Heidelberg; 2016. Available from: https://link.springer.com/article/10.1007/s00468-016-1494-2
4. Patwardhan B, Mashelkar RA. Traditional medicine-inspired approaches to drug discovery: Can Ayurveda show the way forward? Drug Discov Today. 2009 Aug;14(15-16):804-11. doi: 10.1016/j.drudis.2009.05.009, PMID 19477288
5. Heinrich M, Gibbons S. Ethnopharmacology in drug discovery: An analysis of its role and potential contribution. J Pharm Pharmacol. 2001 Apr;53(4):425-32. doi: 10.1211/0022357011775712, PMID 11341358
6. Chen SL, Yu H, Luo HM, Wu Q, Li CF, Steinmetz A. Conservation and sustainable use of medicinal plants: Problems, progress, and prospects. Chin Med. 2016 Jul 30;11:37. doi: 10.1186/s13020-016-0108-7, PMID 27478496, PMCID PMC4967523
7. Flowers of India. *Tiliacora acuminata* (Perungattukodi). Available from: https://www.flowersofindia.net/catalog/slides/tapering-leaf%20tiliacora.html
8. Rodrigues J, Hullatti K, Jalalpure SS, Khanal P. *In vitro* cytotoxicity and *in silico* molecular docking of alkaloids from *Tiliacora acuminata*. Indian J Pharm Educ Res. 2020;54(2 Suppl):S295-S300.
9. Nishanthini A, Mohan VR, Jeeva S. Phytochemical, FT-IR, and GC-MS analysis of STEM and leaf of *Tiliacora Acuminata* (Lan.) Hook F and Thomas (*Menispermaceae*); 2024 Sep 18. Available from: https://ijpsr.com/bft-article/phytochemical-ft-ir-and-gc-ms-analysis-of-stem-and-leaf-of-tiliacora-acuminata-lan-hook-f-thomas-menispermaceae
10. Kumar S. Medico Bio-Wealth of India. Vol. 1. Genève: Zenodo; 2024 Jul 10. doi: 10.5281/zenodo.10251378
11. Grundy SM, Stone NJ, Bailey AL, Beam C, Birtcher KK, Blumenthal RS, *et al*. AHA/ACC/AACVPR/AAPA/ABC/ACPM/ADA/AGS/APhA/ASPC/NLA/PCNA guideline on the management of blood cholesterol: A report of the American College of Cardiology/American heart association task force on clinical practice guidelines. Circulation. 2018 2018 Nov 10:2019 Jun 18;139(25):e1082-43. doi: 10.1161/CIR.0000000000000625. Erratum in: Circulation. e1182-e1186. 2019 Jun 18;139(25). doi: 10.1161/CIR.0000000000000698. Erratum in: Circulation. 2023 Aug 15;148(7):e5. doi: 10.1161/CIR.0000000000001172, PMID 37579012, PMCID PMC7403606
12. Nelson RH. Hyperlipidemia as a risk factor for cardiovascular disease. Prim Care. 2013 Mar;40(1):195-211. doi: 10.1016/j.pop.2012.11.003, PMID 23402469, PMCID PMC3572442.
13. Pradipta S, Wibowo H, Harbuwono DS, Rahajeng E, Larasati RA, Kartika R. Distribution patterns and risk factors of dyslipidemia in patients with type 2 diabetes mellitus: A cross-sectional study in Bogor, Indonesia. Int J Appl Pharm. 2020;12(1):5-8. doi: 10.22159/ijap.2020.v12s1.24045
14. Berta E, Zsíros N, Bodor M, Balogh I, Lőrincz H, Paragh G, *et al*. Clinical aspects of genetic and non-genetic cardiovascular risk factors in familial hypercholesterolemia. Genes. 2022 Jun 27;13:1158.
15. Stroes ES, Thompson PD, Corsini A, Vladutiu GD, Raal FJ, Ray KK, *et al*. Statin-associated muscle symptoms: Impact on statin therapy-European atherosclerosis society consensus panel statement on assessment, aetiology and management. Eur Heart J. 2015 May 1;36(17):1012-22. doi: 10.1093/eurheartj/ehv043, PMID 25694464, PMCID PMC4416140
16. Boekholdt SM, Hovingh GK, Mora S, Arsenault BJ, Amarenco P, Pedersen TR, *et al*. Very low levels of atherogenic lipoproteins and the risk for cardiovascular events: A meta-analysis of statin trials. J Am Coll Cardiol. 2014 Aug 5;64(5):485-94. doi: 10.1016/j.jacc.2014.02.615, PMID 25082583, PMCID PMC4443441
17. Feingold KR. Cholesterol-lowering drugs. In: Feingold KR, Anawalt B, Blackman MR, Boyce A, Chrousos G, Corpas E, editors. Endotext. South Dartmouth, MA: MDText.com, Inc.; 2024 Feb 12. p. 2000, PMID 27809434
18. Hess CN, Low Wang CC, Hiatt WR. PCSK9 inhibitors: Mechanisms of action, metabolic effects, and clinical outcomes. Annu Rev Med. 2018 Jan 29;69:133-45. doi: 10.1146/annurev-med-042716-091351, PMID 29095667
19. Havekes L, Van Hinsbergh V, Kempen HJ, Emeis J. The metabolism *in vitro* of human low-density lipoprotein by the human hepatoma cell line Hep G2. Biochem J. 1983 Sep 15;214(3):951-8. doi: 10.1042/bj2140951, PMID 6312967, PMCID PMC1152337
20. Morris GM, Huey R, Lindstrom W, Sanner MF, Belew RK, Goodsell DS, *et al*. AutoDock4 and AutoDockTools4: Automated docking with selective receptor flexibility. J Comp Chem. 2009;30(16):2785-91. doi: 10.1002/jcc.21256, PMID 19399780
21. Schrödinger LL. PhysiologyMOL Molecular Graphics System. Version 2.0. Schrödinger, LLC.; 2015. Available from: https://github.com/schrodinger/pymol-open-source
22. Tian C, Kasavajhala K, Belfon KA, Raguette L, Huang H, Migues AN, *et al*. ff19SB: Amino-acid-specific protein backbone parameters trained against quantum mechanics energy surfaces in solution. J Chem Theor Comput. 2020 Jan 14;16(1):528-52. doi: 10.1021/acs.jctc.9b00591, PMID 31714766
23. Case DA, Aktulga HM, Belfon K, Cerutti DS, Cisneros GA, Cruzeiro VW, *et al*. AmberTools. J Chem Inf Model. 2023 Oct 23;63(20):6183-91. doi: 10.1021/acs.jcim.3c01153, PMID 37805934, PMCID PMC10598796
24. Eastman P, Swails J, Chodera JD, McGibbon RT, Zhao Y, Beauchamp KA, *et al*. OpenMM 7: Rapid development of high performance algorithms for molecular dynamics. PLoS Comput Biol. 2017 Jul 26;13(7):e1005659. doi: 10.1371/journal.pcbi.1005659, PMID 28746339, PMCID PMC5549999
25. Roe DR, Cheatham TE 3rd. PTRAJ and CPPTRAJ: Software for processing and analysis of Molecular dynamics trajectory data. J Chem Theor Comput. 2013 Jul 9;9(7):3084-95. doi: 10.1021/ct400341p, PMID 26583988
26. Nn A. A review on the extraction methods use in medicinal plants, principle, strength and limitation. Med Aromat Plants. 2015;4:1-6. doi: 10.4172/2167-0412.1000196
27. Ameen F, Alown F, Dawoud T, Sharaf A, Sakayanathan P, Alyahya S. Versatility of copper-iron bimetallic nanoparticles fabricated using *Hibiscus rosa-sinensis* flower phytochemicals: Various enzymes inhibition, antibiofilm effect, chromium reduction and dyes removal. Environ Geochem Health. 2024 Mar 20;46(4):142. doi: 10.1007/s10653-024-01918-3, PMID 38507144
28. Dixon M. The determination of enzyme inhibitor constants. Biochem J. 1953 Aug;55(1):170-1. doi: 10.1042/bj0550170, PMID 13093635, PMCID PMC1269152
29. Lineweaver H, Burk D. The determination of enzyme dissociation constants. J Am Chem Soc. 1934;56(3):658-66. doi: 10.1021/ja01318a036
30. Wang SR, Pessah M, Infante J, Catala D, Salvat C, Infante R. Lipid

and lipoprotein metabolism in Hep G2 cells. Biochim Biophys Acta. 1988 Aug 12;961(3):351-63. Doi: 10.1016/0005-2760(88)90082-3, PMID 3042028

31. Gerlier D, Thomasset N. Use of MTT colorimetric assay to measure cell activation. J Immunol Methods. 1986 Nov 20;94(1-2):57-63. doi: 10.1016/0022-1759(86)90215-2, PMID 3782817
32. Mosmann T. Rapid colorimetric assay for cellular growth and survival: Application to proliferation and cytotoxicity assays. J Immunol Methods. 1983;65(1-2):55-63. doi: 10.1016/0022-1759(83)90303-4, PMID 6606682
33. MTT Cell Proliferation Assay Instruction Guide. ATCC. Available from: https://www.atcc.org
34. Hao S, Xiao Y, Lin Y, Mo Z, Chen Y, Peng X, *et al*. Chlorogenic acid-enriched extract from *Eucommia ulmoides* leaves inhibits hepatic lipid accumulation through the regulation of cholesterol metabolism in hepg2 cells. Pharm Biol. 2016;54(2):251-9. doi: 10.3109/13880209.2015.1029054, PMID 25845641
35. Khera AV, Emdin CA, Drake I, Natarajan P, Bick AG, Cook NR, *et al*. Genetic risk, adherence to a healthy lifestyle, and coronary disease. N Engl J Med. 2016 Dec 15;375(24):2349-58. doi: 10.1056/NEJMoa1605086, PMID 27959714
36. Nishanthini A, Mohan VR. Phytochemical, *in vitro* Antioxidant and Antibacterial Activity of Seed Extracts of *Tiliacora acuminata* (Lan.) Hook F and Thomas (*Menispermaceae*). Available from: https://www.journalijdr.com/phytochemical-vitro-antioxidant-and-antibacterial-activity-seed-extracts-tiliacora-acuminata-lan
37. Simon L, Nanthakumar R, Arumugasamy K. Phytochemical analysis and antimicrobial activity of *Tiliacora acuminata* (Lam.) F. Thoms. (*Menispermaceae*). J Med Plants Stud. 2016;4(6):18-22.
38. Manda RM, Valusa V, Karka SR, Parshaboina VK, Seru G. Evaluation of hypoglycaemic and wound healing activities of *Tiliacora acuminata*. Indian J Pharm Biol Res. 2014;2(4):110-3. doi: 10.30750/ijpbr.2.4.19
39. Duangjai A, Saokaew S. Inhibitory effects of *Tiliacora triandra* (Colebr.) Diels on cholesterol absorption. J Complement Integr Med. 2018 Oct 12;16(1). doi: 10.1515/jcim-2017-0169, PMID 30312160
40. Das G, Gouda S, Kerry RG, Cortes H, Del Prado-Audelo ML, Leyva-Gómez G. Study of traditional uses, extraction procedures, phytochemical constituents, and pharmacological properties of *Tiliacora triandra*. BioMed Res Int. 2022;2022:8754528. doi: 10.1155/2022/8754528
41. Karu N, Reifen R, Kerem Z. Weight gain reduction in mice fed *Panax ginseng* saponin, a pancreatic lipase inhibitor. J Agric Food Chem. 2007 Apr 18;55(8):2824-8. Doi: 10.1021/jf0628025 [ePub]. PMID 17367157.
42. Navarro Del Hierro J, Casado-Hidalgo G, Reglero G, Martin D. The hydrolysis of saponin-rich extracts from fenugreek and Quinoa improves their pancreatic lipase inhibitory activity and hypocholesterolemic effect. Food Chem. 2021 Feb 15;338:128113. doi: 10.1016/j.foodchem.2020.128113, PMID 33092009
43. Li Y, Tran VH, Duke CC, Roufogalis BD. Preventive and protective properties of *Zingiber officinale* (Ginger) in diabetes mellitus, diabetic complications, and associated lipid and other metabolic disorders: A brief review. Evid Based Complement Alternat Med. 2012;2012:516870. doi: 10.1155/2012/516870, PMID 23243452, PMCID PMC3519348
44. Nain CW, Mignolet E, Herent MF, Quetin-Leclercq J, Debier C, Page MM, *et al*. The catechins profile of green tea extracts affects the antioxidant activity and degradation of catechins in DHA-rich oil. Antioxidants (Basel). 2022 Sep 19;11(9):1844. Doi: 10.3390/antiox11091844, PMID 36139917, PMCID PMC9495874
45. Razmpoosh E, Abdollahi S, Mousavirad M, Clark CC, Soltani S. The effects of olive leaf extract on cardiovascular risk factors in the general adult population: A systematic review and meta-analysis of randomized controlled trials. Diabetol Metab Syndr. 2022 Oct 21;14(1):151. doi: 10.1186/s13098-022-00920-y, PMID 36271405, PMCID PMC9585795
46. Kuptawach K, Noitung S, Buakeaw A, Puthong S, Sawangkeaw R, Sangtanoo P, *et al*. Lemon basil seed-derived peptide: Hydrolysis, purification, and its role as a pancreatic lipase inhibitor that reduces adipogenesis by downregulating SREBP-1c and PPAR-γ in 3T3-L1 adipocytes. PLoS One. 2024 May 22;19(5): e0301966. doi: 10.1371/journal.pone.0301966, PMID 38776280, PMCID PMC11111035
47. Ketprayoon T, Noitang S, Sangtanoo P, Srimongkol P, Saisavoey T, Reamtong O, *et al*. An *in vitro* study of lipase inhibitory peptides obtained from de-oiled rice bran. RSC Adv. 2021;11(31):18915-29. doi: 10.1039/D1RA01411K, PMID 35478653
48. Vakele Y, Odun-Ayo F, Reddy L. *In vitro* antioxidant and cytotoxicity activities of selected indigenous South African medicinal plants. Afr Health Sci. 2022 Mar;22(1):395-403. doi: 10.4314/ahs.v22i1.48, PMID 36032452, PMCID PMC9382541
49. Tie F, Ding J, Hu N, Dong Q, Chen Z, Wang H. Kaempferol and Kaempferide attenuate oleic acid-induced lipid accumulation and oxidative stress in HepG2 cells. Int J Mol Sci. 2021;22(16):8847. doi: 10.3390/ijms22168847, PMID 34445549
50. Cui W, Chen SL, Hu KQ. Quantification and mechanisms of oleic acid-induced steatosis in HepG2 cells. Am J Transl Res. 2010;2(1):95-104. PMID 20182586, PMCID PMC2826826
51. James A, Wang K, Wang Y. Therapeutic activity of green tea epigallocatechin-3-gallate on metabolic diseases and non-alcoholic fatty liver diseases: The current updates. Nutrients. 2023 Jul 3;15(13):3022. doi: 10.3390/nu15133022, PMID 37447347, PMCID PMC10346988